MR No. E5J04

NATIONAL ADVISORY COMMITTEE FOR AERONAUTICS

WARTIME REPORT

ORIGINALLY ISSUED

October 1945 as
Memorandum Report E5J04

CORRELATION OF THE CHARACTERISTICS OF SINGLE-CYLINDER AND FLIGHT ENGINES IN TESTS OF HIGH-PERFORMANCE FUELS IN AN AIR-COOLED ENGINE

I - COOLING CHARACTERISTICS

By Robert W. Wilson, Paul H. Richard, and Kenneth D. Brown

Aircraft Engine Research Laboratory
Cleveland, Ohio

NACA

WASHINGTON

NACA MR No. E5J04

NATIONAL ADVISORY COMMITTEE FOR AERONAUTICS

MEMORANDUM REPORT

for the

Air Technical Service Command, Army Air Forces

CORRELATION OF THE CHARACTERISTICS OF SINGLE-CYLINDER AND FLIGHT ENGINES IN TESTS OF HIGH-PERFORMANCE FUELS IN AN AIR-COOLED ENGINE

I - COOLING CHARACTERISTICS

By Robert W. Wilson, Paul H. Richard, and Kenneth D. Brown

SUMMARY

Variable charge-air flow, cooling-air pressure drop, and fuel-air ratio investigations were conducted to determine the cooling characteristics of a full-scale air-cooled single cylinder on a CUE setup. The data are compared with similar data that were available for the same model multicylinder engine tested in flight in a four-engine airplane.

The cylinder-head cooling correlations were the same for both the single-cylinder and the flight engine. The cooling correlations for the barrels differed slightly in that the barrel of the single-cylinder engine runs cooler than the barrel of the flight engine for the same head temperatures and engine conditions.

INTRODUCTION

At the request of the Air Technical Service Command, Army Air Forces, an investigation is being conducted at the NACA Cleveland laboratory to evaluate triptane and other high antiknock additives as blending agents of aviation fuels. A part of this program is to correlate the knock-limited and cooling-limited performances of a single cylinder on a CUE setup with those of a multicylinder engine in flight.

The relation of the knock limit to the cooling limit is important in predicting the maximum safe engine performance. Whereas the knock limits of the single-cylinder and flight engines may match, the cooling limit of the single-cylinder engine could be very different from that of the flight engine. The knock-limited performance of the single-cylinder and flight engines compared under a variety of engine operating conditions is reported in part II.

The cooling characteristics of the flight engine are presented in reference 1. The tests presented in this report were conducted at the NACA Cleveland laboratory during April 1945 and permit the study of the single-cylinder cooling by the NACA cooling-correlation equations.

INSTRUMENTATION

An attempt was made in the single-cylinder tests to simulate just as closely as possible all the conditions of the flight tests reported in reference 1, with which the single-cylinder data obtained in these tests were to be correlated. A front-row cylinder for the same model engine was used in the setup shown in figure 1. The compression ratio in both cases was 6.7. A vaporization tank was installed in the single-cylinder setup (fig. 2) to simulate the mixing and vaporizing of the fuel in the flight engine. A standard engine intake pipe was installed to represent the induction system of the flight engine. The fuel was 28-R in both series of tests.

The location of thermocouples and pressure tubes in the flight tests is set forth in detail in the appendix of reference 1. The locations were kept as nearly as possible the same in the single-cylinder setup. The cooling-air pressure distribution that would be encountered in flight was simulated by cooling-air turbulence vanes in front of the single cylinder. Cylinder temperatures were measured by iron-constantan thermocouples located at the rear-spark-plug gasket, the front-spark-plug boss, the rear-spark-plug boss, the rear middle barrel, and the rear flange. The mixture temperature in both cases was measured by an unshielded iron-constantan thermocouple installed in the center of the 90° elbow of the intake pipe. In the flight tests the mixture and cylinder temperatures were determined from an average of the 14 cylinders. The cooling-air pressure drop across the single cylinder for both the cylinder heads and barrels was determined from the differential of the total pressure ahead of the cylinder and the static pressure at the rear of the cylinder. The cooling-air pressure was corrected to a standard air density of 0.002378 slug per cubic foot ahead of the cylinder.

The cold valve clearances for the single-cylinder engine were set at 0.090 inch for the intake valve and 0.060 inch for the exhaust valve. These valve clearances were found in a previous investigation (reference 2) on the same single-cylinder setup to give a running valve timing close to that specified for the multicylinder engine (intake opens, 36° B.T.C.; intake closes, 60° A.B.C.; exhaust opens, 76° B.B.C.; exhaust closes, 20° A.T.C.). The cold valve clearances for the flight engine were set at 0.020 inch as specified by the engine manufacturer.

TEST PROCEDURE

Three types of cooling test were run to obtain single-cylinder data to compare with the cooling data for the flight engine presented in reference 1. The charge-air flow, the cooling-air pressure drop, and the fuel-air ratio were independently varied and at conditions very closely matching those of the flight-engine tests. The engine operating conditions that were used in the single-cylinder tests are presented in the following table:

SINGLE-CYLINDER ENGINE OPERATING CONDITIONS

[Engine speed, 2250 rpm; spark advance, 25° B.T.C.; cooling-air temperature ahead of cylinder, T_a, 58° F.]

Engine Conditions	Test variables		
	Charge-air flow	Cooling-air pressure drop	Fuel-air ratio
Charge-air flow, M_a, lb/hr-cylinder	Varied	405	413
Cooling-air pressure drop, in. water:			
Head $\sigma\Delta p_h$	11.6	Varied	11.8
Barrel $\sigma\Delta p_b$	10.7	Varied	11.0
Fuel-air ratio	0.080	0.080	Varied
Dry inlet-air temperature, °F	200	200	180

RESULTS AND DISCUSSION

Comparison of engine temperatures. - Figures 3, 4, and 5 are a presentation of cylinder temperatures and engine performance against charge-air flow, cooling-air pressure drop, and fuel-air ratio, respectively, for the single-cylinder and flight engines. The

cylinder-head temperatures for the single-cylinder and flight engines match very well, but the cylinder-barrel temperatures for the single-cylinder engine are lower than for the flight engine. Single-cylinder engine performance is presented on an indicated basis and flight engine performance (from reference 1) is presented on a brake basis. The cooling-air-pressure distribution for the two engines was not the same in that the pressures were higher for the barrels and lower for the heads of the single-cylinder engine than for the flight engine.

In order to compare the cylinder temperatures for the single-cylinder and flight engines the difference in the cooling-air temperature ahead of the cylinder T_a, for the single-cylinder and flight engines (18° F) was added to the cylinder temperatures of the flight engine. The cooling-air temperature ahead of the cylinder T_a, for the single-cylinder engine was 58° F and for the flight engine was 40° F.

In figures 3, 4, and 5 the manifold pressures of the single-cylinder and the flight engines differ in that the points of measurement were different.

Figures 6 and 7 show that for the single-cylinder and flight engines the rear-spark-plug boss and the rear middle-barrel temperatures have the same relation to the rear-spark-plug gasket and the rear flange temperatures, respectively. In figure 7 there is no straight-line relation between the temperatures for the variable cooling-air pressure drop runs but the temperatures for the single-cylinder and flight engines fall on the same curve.

Comparison of engine cooling by the NACA correlation method. - The NACA cooling-correlation equations as used for the flight engine (reference 1) are as follows:

$$\frac{T_h - T_a}{T_{g_h} - T_h} = K\left(\frac{W_c^{n/m}}{\sigma \Delta p_h}\right)^m$$

and

$$\frac{T_b - T_a}{T_{g_b} - T_b} = K\left(\frac{W_c^{n/m}}{\sigma \Delta p_b}\right)^m$$

where

T_h average cylinder-head temperature, °F

T_b average cylinder-barrel temperature, °F

T_a cooling-air temperature ahead of cylinder, °F

T_{g_h}, T_{g_b} mean effective gas temperature for head and barrel, respectively, °F

W_c charge-air flow (on flight-engine basis), $\frac{\text{pounds/hour}}{1000}$

σ ratio of cooling-air density ahead of cylinder to standard air density of 0.002378 slug/cu ft

Δp_h, Δp_b cooling-air pressure drop for head and barrel, respectively, in. water

n, m, k empirical constants

For the cooling correlation presented in this report the rear-spark-plug boss and the rear middle-barrel temperatures were used as an indication of T_h and T_b, respectively.

Following the procedure used in roferences 1 and 3, variations of T_g with changes in dry inlet-charge temperatures are acccunted for by using a reference mean effective gas temperature T_{g_o} for a dry inlet-charge temperature of 0° F and the following equations (from reference 4):

$$T_{g_h} = T_{g_{o_h}} + 0.8\, T_m$$

$$T_{g_b} = T_{g_{o_b}} + 0.42\, T_m$$

where

T_m dry inlet-charge temperature, °F

$T_{g_{o_h}}$, $T_{g_{o_b}}$ reference mean effective gas temperature for head and barrel, respectively, °F (T_m = 0° F) T_{g_o} is solely a function of fuel-air ratio in these tests.

In the correlation for the single-cylinder engine the same values of $T_{g_{o_h}}$ and $T_{g_{o_b}}$ (1086° and 536° F, respectively, at a fuel-air ratio of 0.080) were used as in references 1 and 3.

The values of the constants n, m, and k in the correlation equations were determined from the variable charge-air flow and cooling-air pressure drop tests at a fuel-air ratio of 0.080. The variation of $T_{g_{o_h}}$ and $T_{g_{o_b}}$ with fuel-air ratio was then determined from the variable fuel-air ratio tests.

The exponent n that governs the effect of charge-air flow on the functions $\frac{T_h - T_a}{T_{g_h} - T_h}$ and $\frac{T_b - T_a}{T_{g_b} - T_b}$ is evaluated from the slopes of the plots shown in figure 8.

The exponent m that governs the effect of cooling-air pressure drop on the functions $\frac{T_h - T_a}{T_{g_h} - T_h}$ and $\frac{T_b - T_a}{T_{g_b} - T_b}$ is evaluated from the slopes of the plots shown in figure 9.

Final cooling-correlation lines for heads and barrels of the single-cylinder and flight engines were obtained by using the exponents determined from the plots shown in figures 8 and 9 and by plotting $\frac{T_h - T_a}{T_{g_h} - T_h}$ and $\frac{T_b - T_a}{T_{g_b} - T_b}$ against $\frac{W_c^{n/m}}{\sigma \Delta p}$ (fig. 10). The cooling equations obtained were as follows:

For heads, single-cylinder and flight engines:

$$\frac{T_h - T_a}{T_{g_h} - T_h} = 0.270 \left(\frac{W_c^{2.134}}{\sigma \Delta p_h} \right)^{0.320}$$

For barrels, single-cylinder engine:

$$\frac{T_b - T_a}{T_{g_b} - T_b} = 0.340 \left(\frac{W_c^{1.614}}{\sigma \Delta p_b} \right)^{0.438}$$

For barrels, flight engine:

$$\frac{T_b - T_a}{T_{g_b} - T_b} = 0.505 \left(\frac{W_c^{1.309}}{\sigma \Delta p_b} \right)^{0.567}$$

For the single-cylinder and flight engines the constants in the equation for the heads are the same, which indicates the same relation of head temperature to change in power and cooling-air pressure drop with other conditions the same. The constants in the equation for the barrels are, however, different for the two conditions because the barrel of the single-cylinder engine runs cooler than the barrel of the flight engine for the same power and cooling-air pressure drop.

Figure 11 is a plot of T_{g_o} against fuel-air ratio for the heads and barrels of the single-cylinder and the flight engines. The T_{g_o} curves for the flight engine were obtained from data at a wide variety of engine conditions. (See references 1 and 3.) The T_{g_o} curves for the single-cylinder and flight engines match fairly well.

SUMMARY OF RESULTS

The cylinder-head cooling correlations were the same for both the single-cylinder and the flight engines. The cooling correlations for the barrels differed slightly in that the barrel of the single-cylinder engine runs cooler than the barrel of the flight engine for the same head temperatures and engine conditions.

Aircraft Engine Research Laboratory,
National Advisory Committee for Aeronautics,
Cleveland, Ohio, October 4, 1945.

REFERENCES

1. Werner, Milton, Blackman, Calvin C., and White, H. Jack: Flight and Test-Stand Investigation of High-Performance Fuels in Modified Double-Row Radial Air-Cooled Engines. I - Determination of the Cooling Characteristics of the Flight Engine. NACA MR No. E5G09, 1945.

2. Cook, Harvey A., Richard, Paul H., and Brown, Kenneth D.: The Effect of Valve Clearance on Knock-Limited Performance and Engine Cooling. NACA MR No. E5D18, 1945.

3. White, H. Jack, Blackman, Calvin C., and Dandois, Marcel: Flight and Test-Stand Investigation of High-Performance Fuels in Double-Row Radial Air-Cooled Engines. III - Comparison of Cooling Characteristics of Flight and Test-Stand Engines. NACA MR No. E5B23, 1945.

4. Corson, Blake W., Jr., and McLellan, Charles H.: Cooling Characteristics of a Pratt & Whitney R-2800 Engine Installed in an NACA Short-Nose High-Inlet-Velocity Cowling. NACA ACR No. L4F06, 1944.

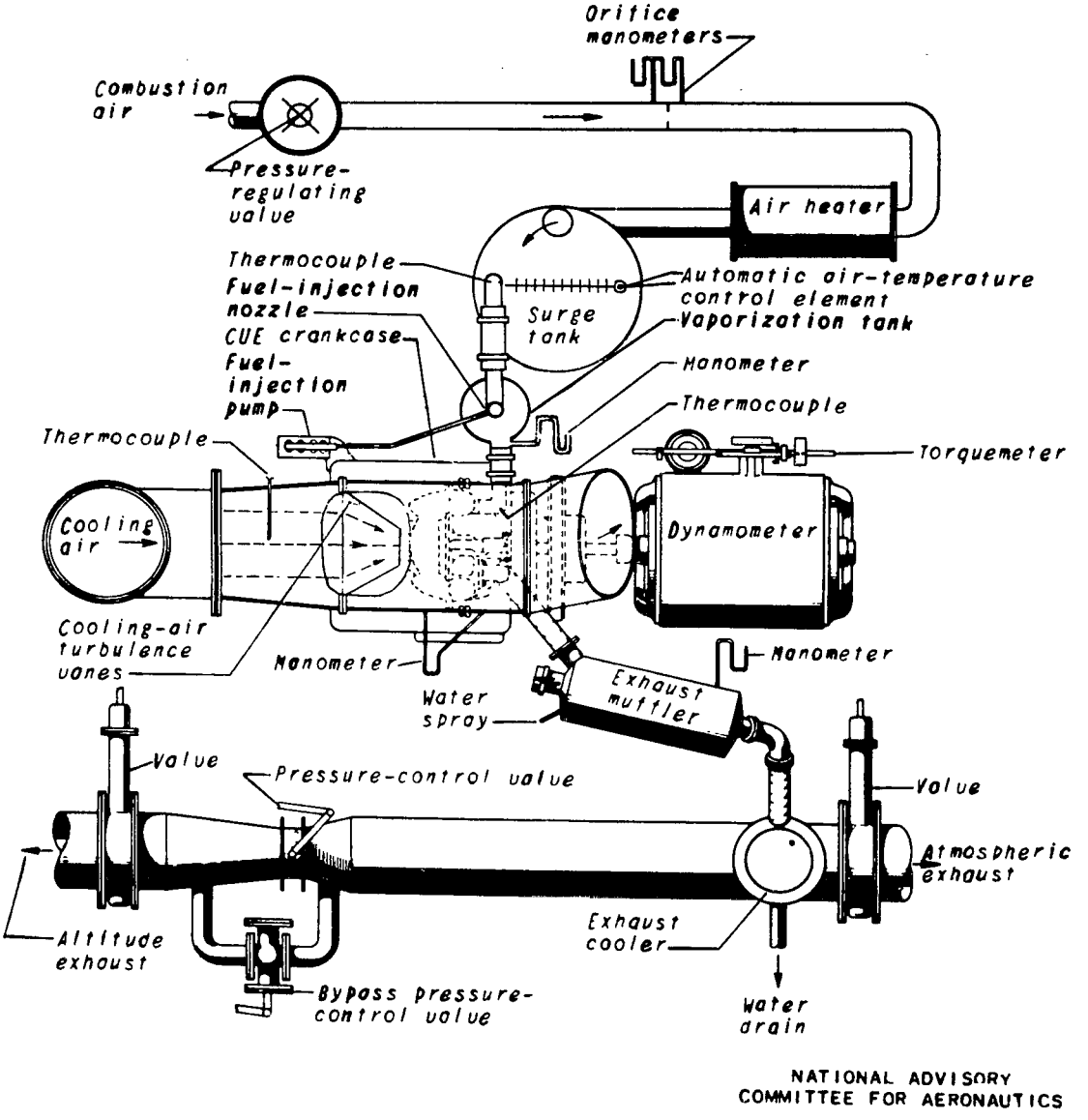

Figure 1. - Air-cooled single-cylinder setup.

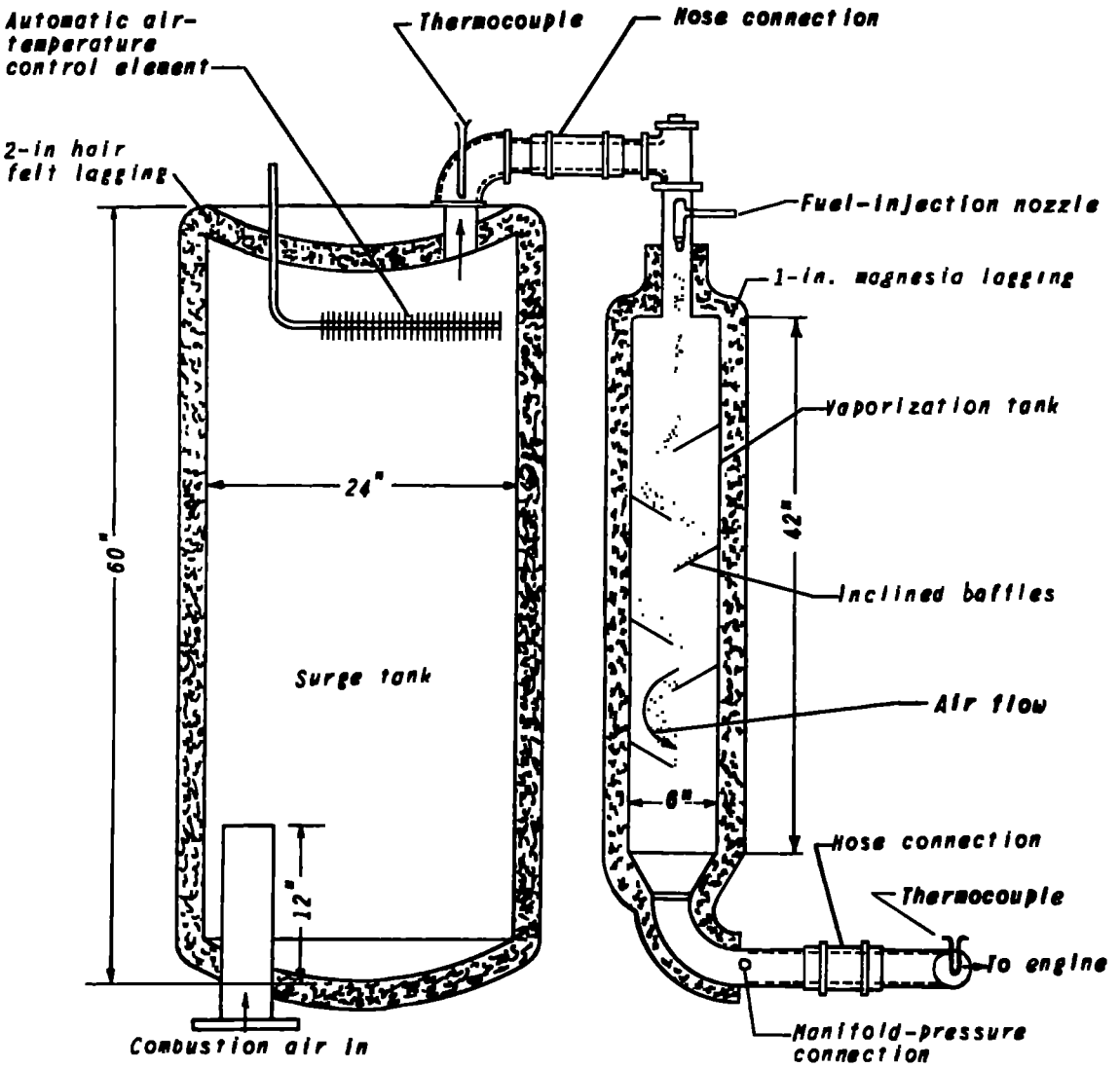

Figure 2. – Induction system used in single-cylinder setup.

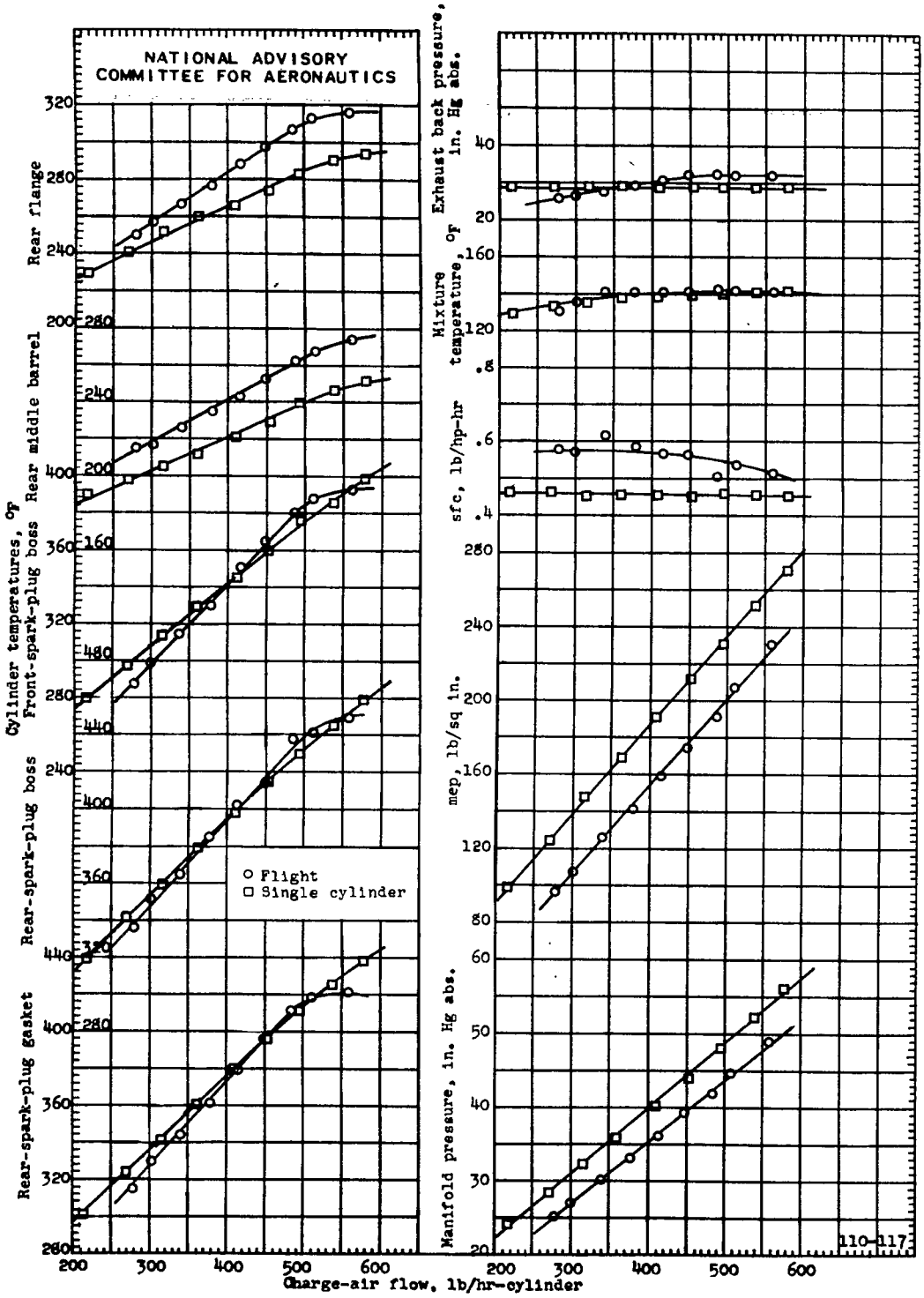

Figure 3. - Variation of cylinder temperatures and engine performance with charge-air flow for the single-cylinder and flight engines. Single-cylinder engine performance is presented on an indicated basis and flight engine performance (reference 1) is presented on a brake basis. Engine speed, 2250 rpm; compression ratio, 6.7; spark advance, 25° B.T.C.; fuel, 28-R; fuel-air ratio, 0.080; single-cylinder cooling-air pressure drop, $c\Delta p_h$, 11.6 in. H_2O; $c\Delta p_b$, 10.7 in. H_2O; flight cooling-air pressure drop, $c\Delta p_h$, 11.8 in. H_2O; $c\Delta p_b$, 10.1 in. H_2O.

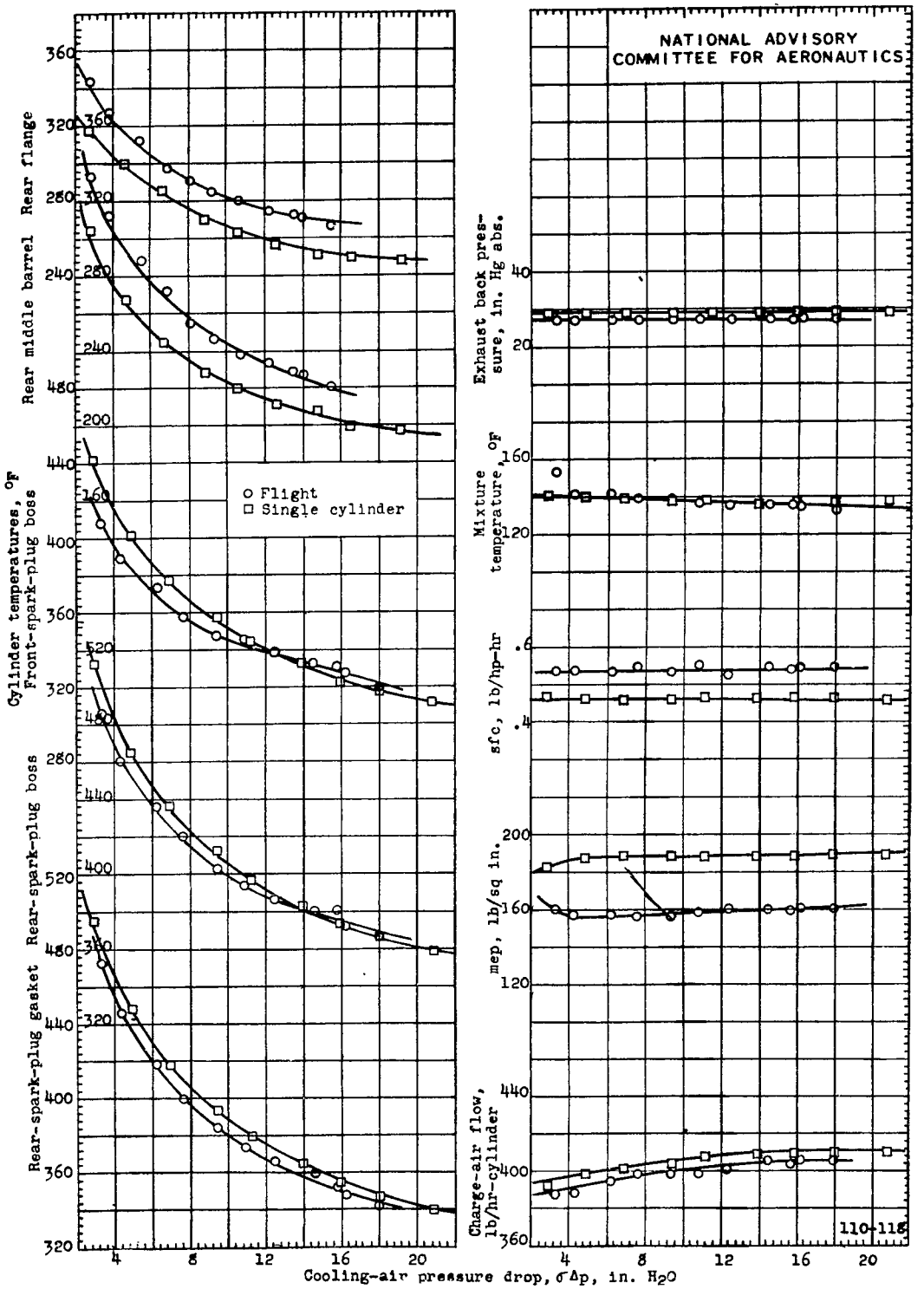

Figure 4. - Variation of cylinder temperatures and engine performance with cooling-air pressure drop for the single-cylinder and flight engines. Single-cylinder engine performance is presented on an indicated basis and flight engine performance (reference 1) is presented on a brake basis. Head temperatures are plotted against head σΔp and barrel temperatures are plotted against barrel σΔp. Engine speed, 2250 rpm; compression ratio, 6.7; spark advance, 25° B.T.C.; fuel, 28-R; fuel-air ratio, 0.080; single-cylinder manifold pressure, 40.0 in. Hg abs.; flight manifold pressure, 35.0 in. Hg abs.

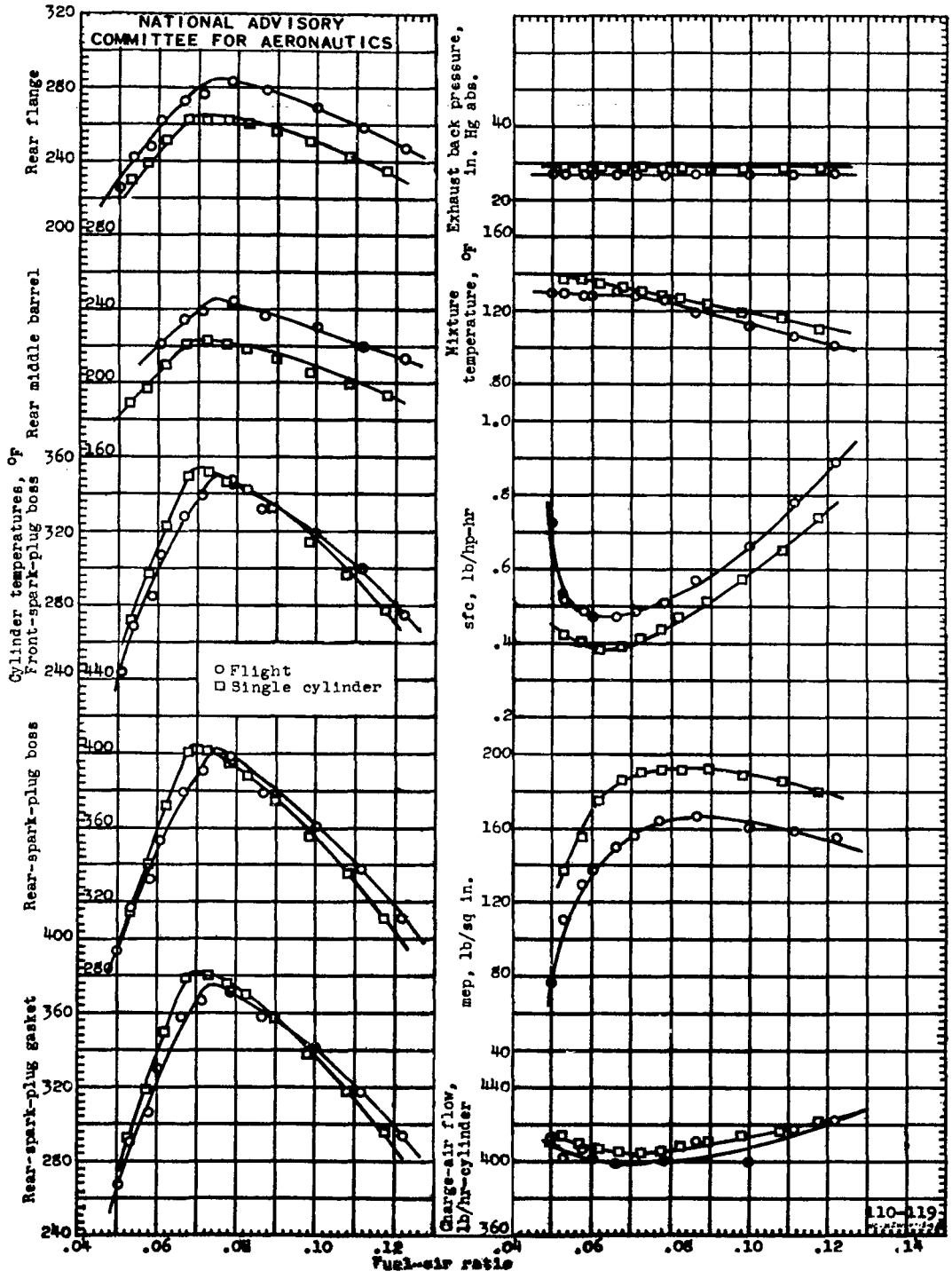

Figure 5. - Variation of cylinder temperatures and engine performance with fuel-air ratio for the single-cylinder and flight engines. Single-cylinder engine performance is presented on an indicated basis and flight engine performance (reference 1) is presented on a brake basis. Engine speed, 2250 rpm; compression ratio, 6.7; spark advance, 25° B.T.C.; fuel, 28-R; single cylinder: cooling-air pressure drop, $c\Delta p_h$, 11.8 in. H_2O; $c\Delta p_b$, 11.0 in. H_2O; manifold pressure, 39.6 in. Hg abs.; flight: cooling-air pressure drop, $c\Delta p_h$, 12.2 in. H_2O; $c\Delta p_b$, 10.4 in. H_2O; manifold pressure, 35.2 in. Hg abs.

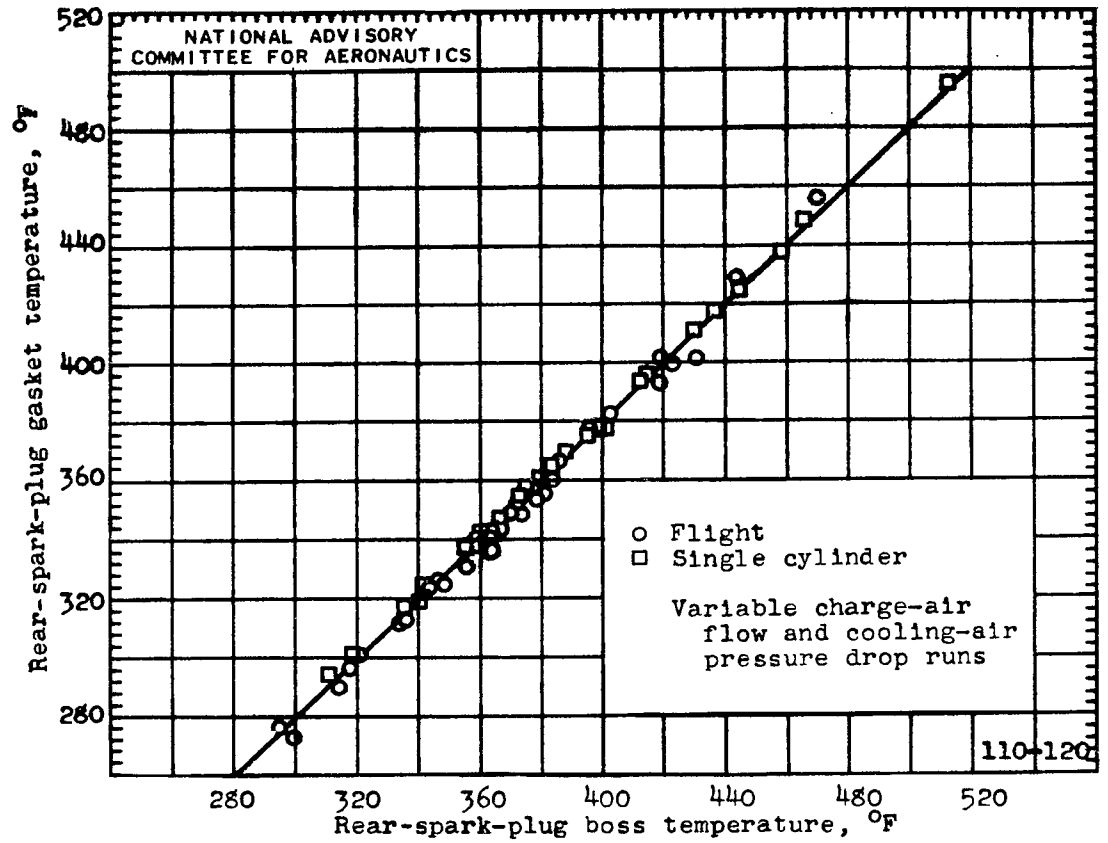

Figure 6. - Comparison of rear-spark-plug gasket temperature with rear-spark-plug boss temperature for the single-cylinder and the multi-cylinder engine. Engine speed, 2250 rpm; compression ratio, 6.7; spark advance, 25° B.T.C.; fuel, 28-R; fuel-air ratio, 0.080.

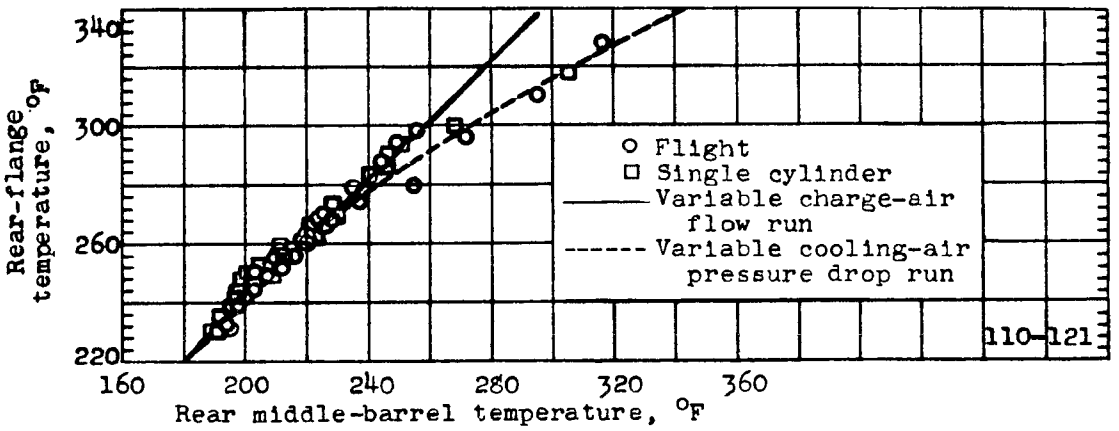

Figure 7. - Comparison of rear-flange temperature with rear middle-barrel temperature for the single-cylinder and flight engines. Engine speed, 2250 rpm; compression ratio, 6.7; spark advance, 25° B.T.C.; fuel, 28-R; fuel-air ratio, 0.080.

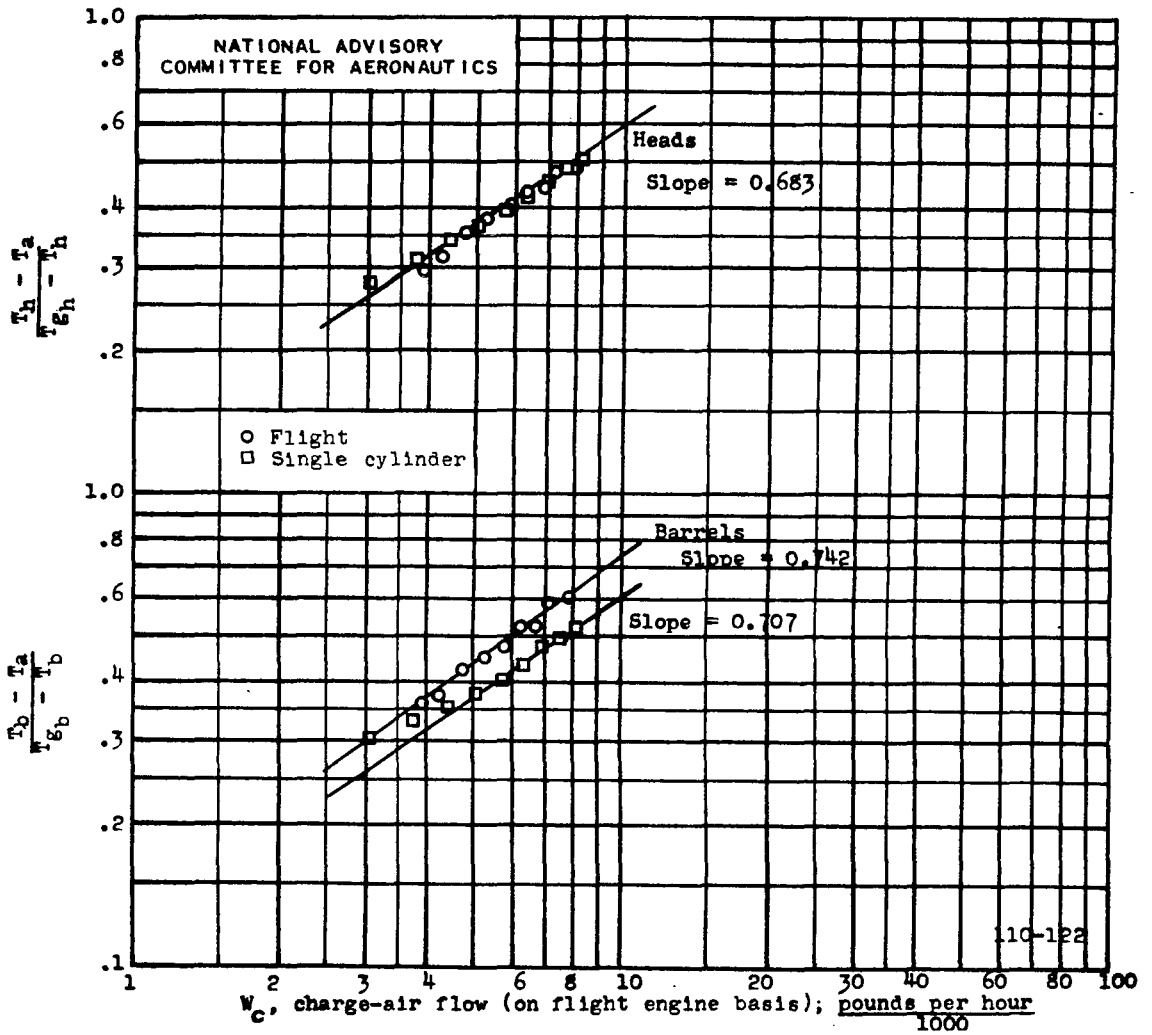

Figure 8. - Variation of $\frac{T_h - T_a}{T_{g_h} - T_h}$ and $\frac{T_b - T_a}{T_{g_b} - T_b}$ with charge-air flow, W_c, for the single-cylinder and flight engines. Engine speed, 2250 rpm; compression ratio, 6.7; spark advance, 25° B.T.C.; fuel, 28-R; fuel-air ratio, 0.080; cooling-air pressure drop: $\sigma\Delta p_h$, 11.6 in. H_2O; $\sigma\Delta p_b$, 10.7 in. H_2O.

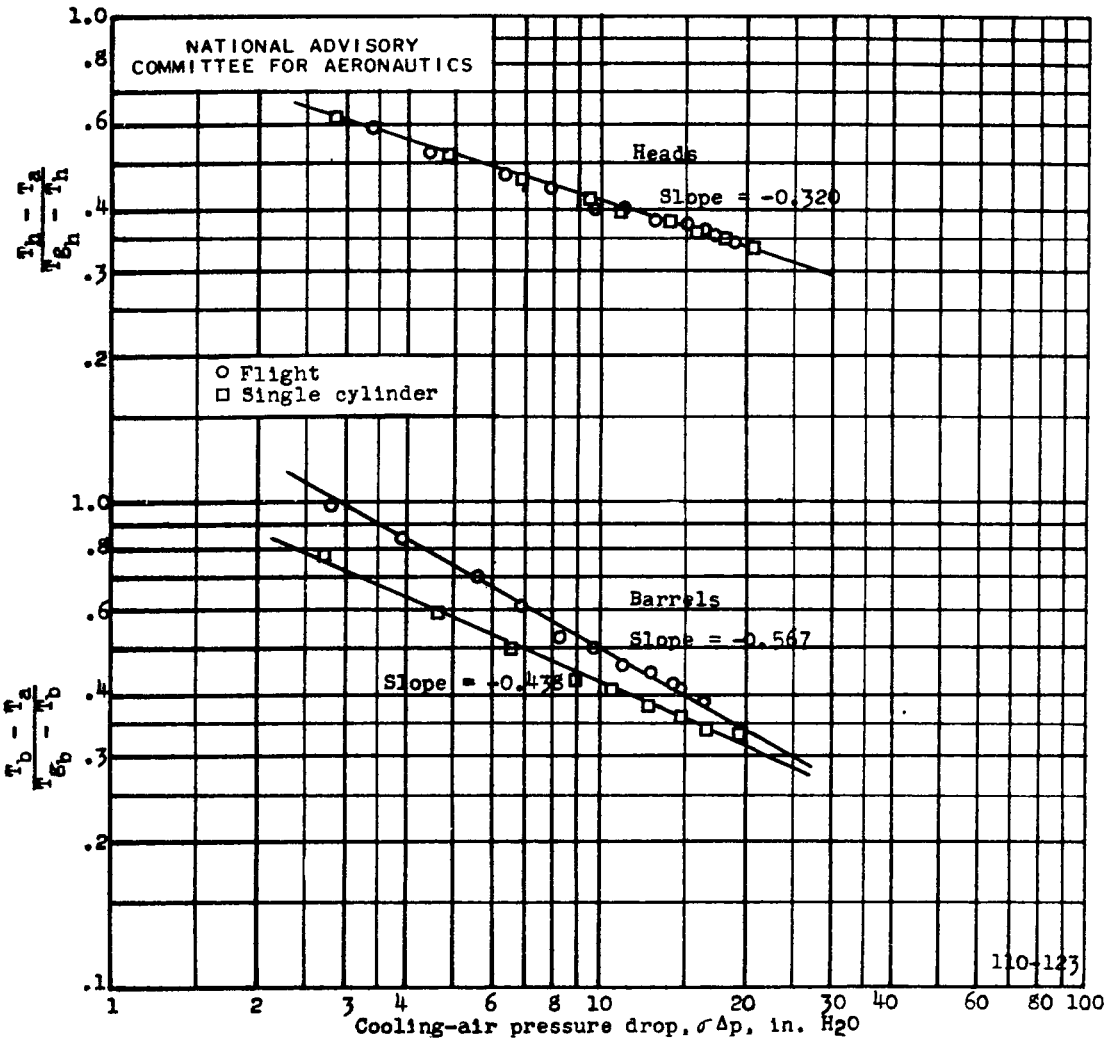

Figure 9. - Variation of $\frac{T_h - T_a}{T_{g_h} - T_h}$ and $\frac{T_b - T_a}{T_{g_b} - T_b}$ with cooling-air pressure drop for the single-cylinder and flight engines. Engine speed, 2250 rpm; compression ratio, 6.7; spark advance, 25° B.T.C.; fuel, 28-R; fuel-air ratio, 0.080; charge-air flow, 405 lb/hr-cylinder.

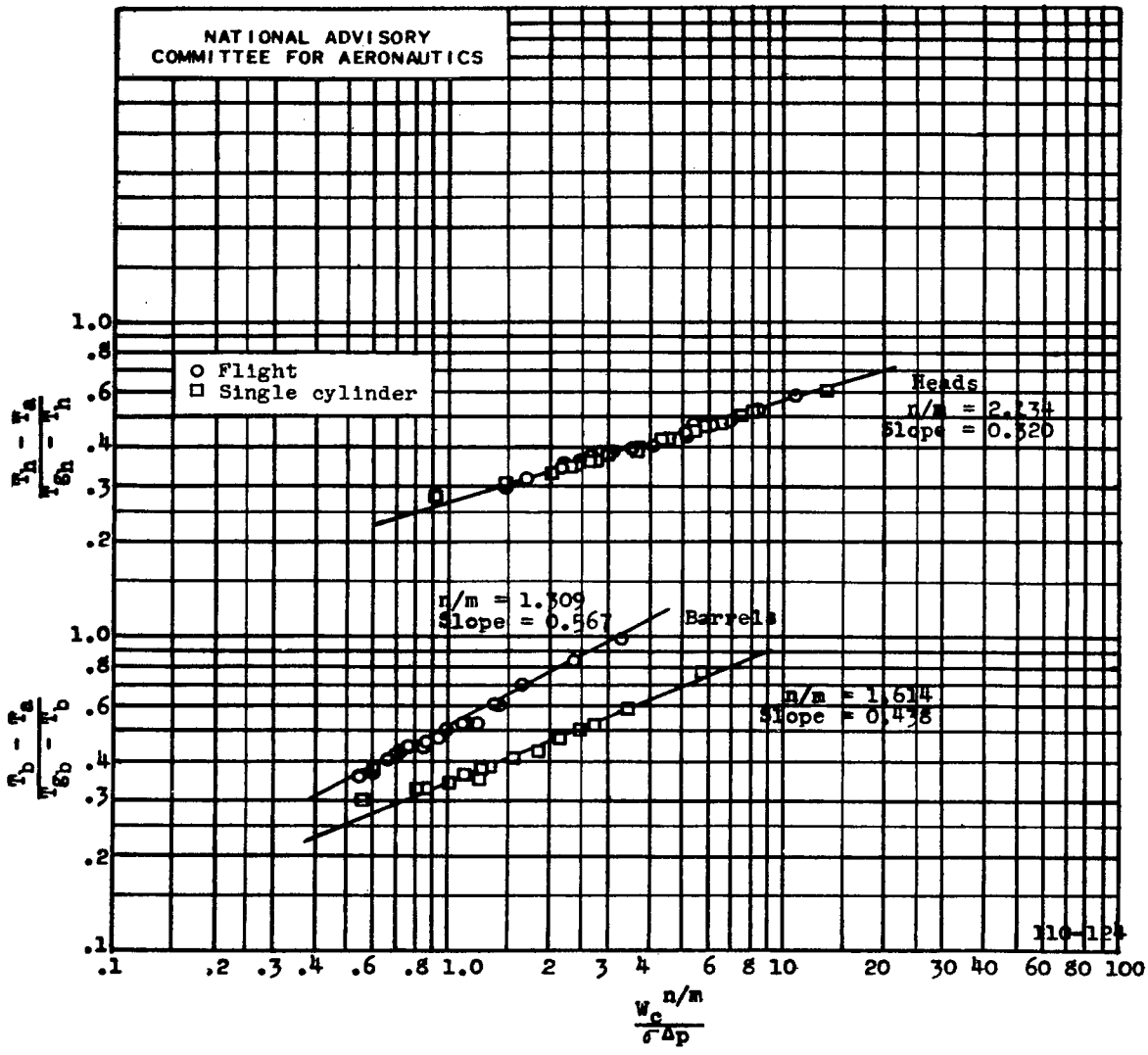

Figure 10. - Cooling-correlation curves for the single-cylinder and flight engines. Engine speed, 2250 rpm; compression ratio, 6.7; spark advance, 25° B.T.C.; fuel, 28-R; fuel-air ratio, 0.080.

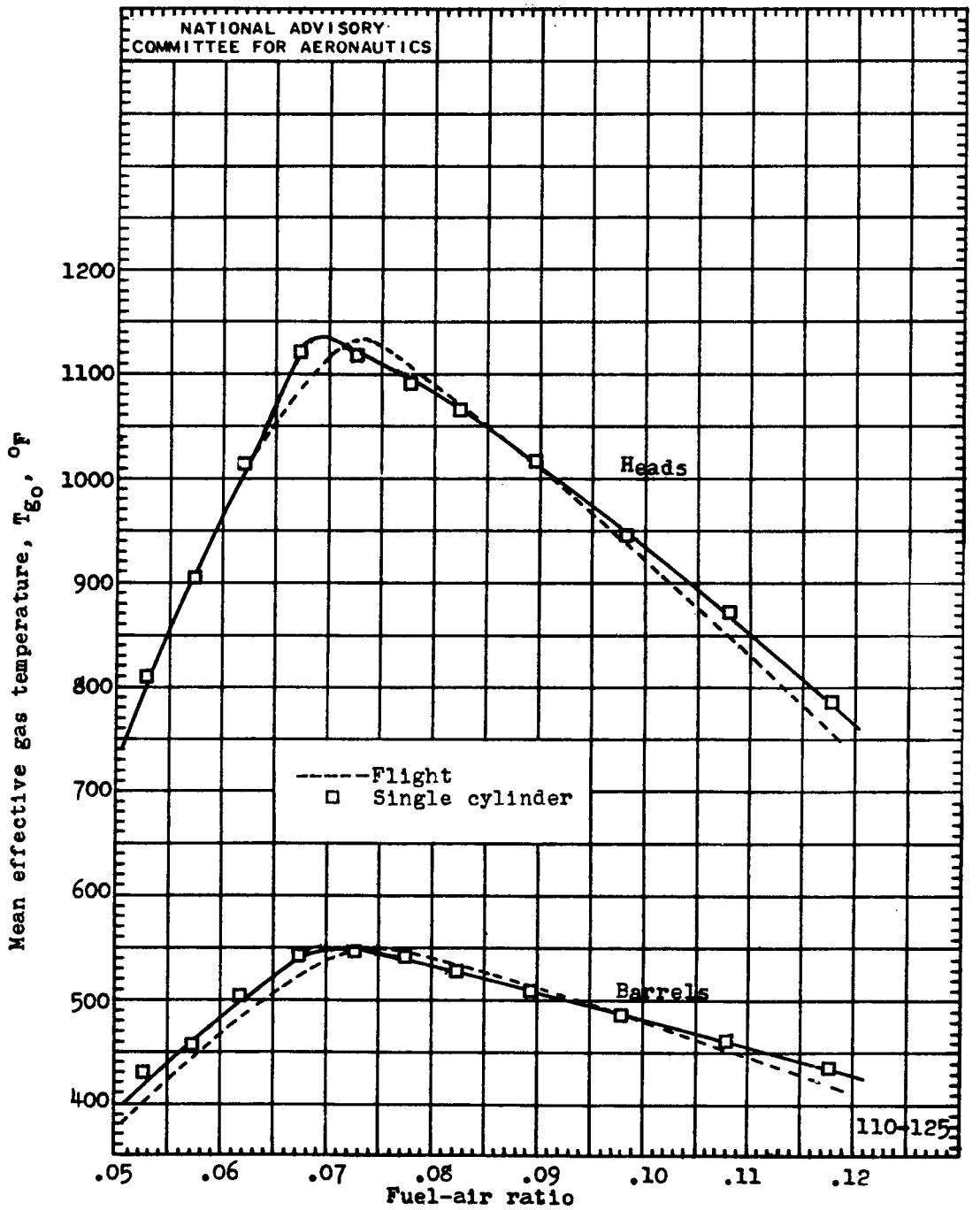

Figure 11. - Variation of mean effective gas temperature T_{g_o} with fuel-air ratio for the single-cylinder and flight engines. Engine speed, 2250 rpm; compression ratio, 6.7; spark advance, 25° B.T.C.; fuel, 28-R.